JMEPEG (2006) 15:145-148
DOI: 10.1361/105994906X95788

1059-9495/$19.00

Liquid Impact Erosion of Single-Crystal and Coated Materials

M.J. Jackson, R.H. Telling, and J.E. Field

(Submitted November 4, 2005; in revised form December 19, 2005)

Lithium fluoride in its single-crystal form is an interesting material for investigating the development of fracture by multiple liquid impact owing to its well-characterized crystal structure. The development of fracture during liquid impact is attributed to the extension of short circumferential cracks produced around the loaded area by the passing Rayleigh stress wave after the impact event. The damage threshold of single-crystal lithium fluoride is developed using the multiple-impact jet apparatus (MIJA) as a result of identifying the characteristic fracture annulus associated with liquid impact during a controlled experimental procedure. The observation of damage produced in solids by liquid impact has practical significance in the problems associated with supersonic aircraft flying through rain and in the erosion of turbine blades. The addition of coatings to the surface provides a form of protection at higher speeds but may not completely inhibit damage.

Keywords coatings, fracture, liquid impact, single crystals, surface characterization, surface damage

1. Nature of Impact Damage

Liquid impact on single-crystal materials was first reported by Jolliffe (Ref 1). Jolliffe impacted single-crystal magnesium oxide (MgO) with methanol, water, oil, and mercury droplets then etched them to reveal dislocation activity. However, Jolliffe did not impact single-crystal MgO beyond its damage threshold velocity but did induce the movement of dislocations. Jolliffe noted that dislocation movement due to repeated impact by liquids is caused by the extension of dislocation loops to form slip bands on $\{110\}_{45^\circ}$ planes. Research workers at the Cavendish Laboratory (Ref 2) noticed that the nature of impact damage in single-crystal MgO due to liquid impact was in the form of slip bands in the $\langle 100 \rangle$ direction until the material reached its damage threshold limit. Figure 1 shows an image of the impact zone showing dislocation slip and movement prior to fracture. When the limit was reached, {110}-type cracks appeared in the $\langle 100 \rangle$ direction, which were presumably formed by the interaction of $\{110\}_{45^\circ}$ slip planes. Further studies have revealed a number of important fracture observations in multiple liquid impact experiments.

In addition to the characteristic slip-band pattern for single- and multiple-liquid impacts on (001) MgO, there is a fracture annulus surrounding the central impact zone. When etched and viewed in reflected illumination, the crack types within the fracture annulus have the following characteristics:

- (Type I) Due to fourfold symmetry around the [001] impact axis, the damage is the same in eight octants.
- (Type II) Cracks exist in an annulus whose boundary is square in shape with a slight tendency to be elliptical. The diagonals associated with this annulus are the [010] and [100] directions.
- (Type III) Cracks at the release radius are very short in length.
- (Type IV) Within the $\langle 100 \rangle$ radial direction, larger cracks intersect the surface tangent to the impact release radius.
- (Type V) Cracks located near to $\langle 110 \rangle$ radial direction are of two varieties: those that intersect on the (001) impact face, and those that are apparent distortions in the radial direction of type II fractures. Intersections of these cracks from two quadrants form W-shaped cracks.

These characteristic crack types have been identified in single-impact water-drop experiments (Ref 3). Cracks found immediately at the release radius are short in depth (less than 5 μm)

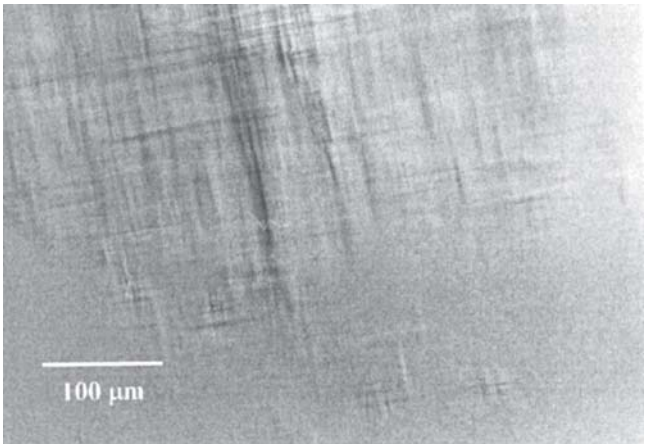

Fig. 1 Impact zone on (001) surface of single-crystal MgO showing dislocation movement prior to fracture

This paper was presented at the fourth International Surface Engineering Congress and Exposition held August 1-3, 2005 in St. Paul, MN.

M.J. Jackson, Center for Advanced Manufacturing, College of Technology, Purdue University, West Lafayette, IN 47907; and **R.H. Telling** and **J.E. Field,** Cavendish Laboratory, University of Cambridge, Madingley Road, Cambridge, CB3 0HE, U.K. Contact e-mail: jacksomj@purdue.edu.

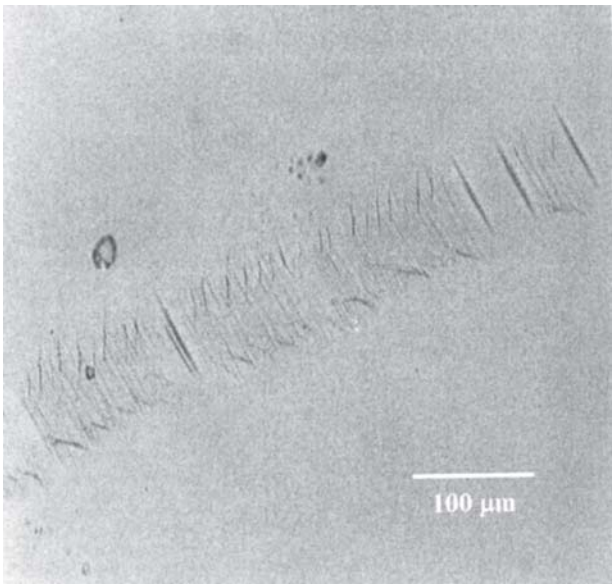

Fig. 2 Minor damage to the (001) surface of MgO caused by lateral jetting of the water drop

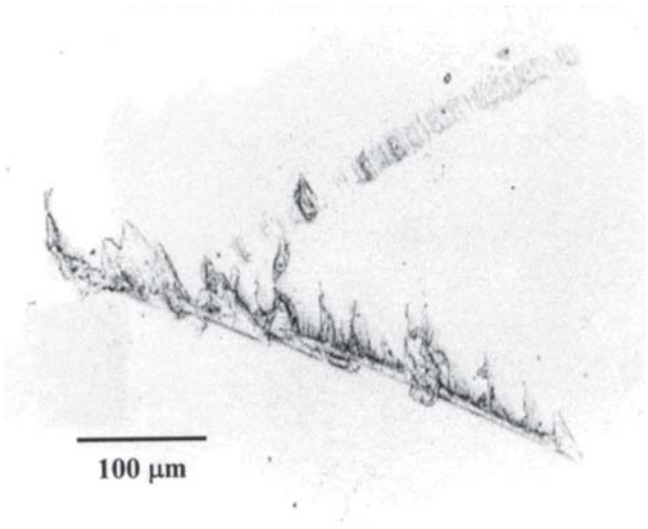

Fig. 3 Major damage to the (001) surface of MgO caused by lateral jetting of the water drop

Table 1 Properties of single-crystal lithium fluoride

Property	Magnitude
Young's modulus, $E_{\langle 100\rangle}$, MPa	64.8
Poisson's ratio, $\nu_{\langle 100\rangle}$	0.27
Density, ρ, kg/m^{-3}	2600
Fracture toughness, $K_{Ic\langle 100\rangle}$, MPa$\sqrt{m}$	0.2
Slip system	$\{110\}\langle 1\bar{1}0\rangle$
Cleavage plane	{100}
Water solubility, mg/100 g water	270
Knoop hardness, kg/mm^2	
(001) ⟨100⟩	87-96
(001) ⟨110⟩	93-103
$(1\bar{1}0)\langle 001\rangle$	87-98
$(1\bar{1}0)\langle 1\bar{1}1\rangle$	97-120
(110) ⟨110⟩	93-116

and are thought to be cracks introduced by polishing that are excited by the passing Rayleigh wave. The onset of visible cracking at the release radius was used as a measure of the damage threshold of the material at a known impact velocity. This tends to give a conservative estimate of the absolute damage threshold of the material. Lateral jetting of the water drop tends to produce secondary fractures that have been excited by the passing Rayleigh wave. These secondary fractures cause further damage to the surface of the material and can induce minor damage (Fig. 2) or significant damage (Fig. 3) to the surface of the single crystal material.

2. Experimental Procedures

Crystran Ltd. (Dorset, U.K.) supplied single crystals of lithium fluoride as undoped high-purity single crystals. Crystran prepared the specimens for impact experiments by cleaving and polishing the crystals. The crystals were cleaved to size on {100} planes and mechanically polished on one side to remove cleavage steps. Chemical polishing was performed to remove mechanically induced polishing dislocations from the surface of the crystal. This was achieved by immersing the crystals in a bath of hydrochloric acid (HCl) at 50 °C followed by immersion in ammonium chloride (NH_4Cl) to remove etch pits. A light mechanical polish using 0.25 μm diamond paste followed immersion to obtain a clean surface. The surfaces were then orientated to within 2° of a {100} plane. The impact face was denoted the (001) plane. The properties of single-crystal lithium fluoride are shown in Table 1.

The apparatus used to simulate rain erosion is the multiple-impact jet apparatus (MIJA). The apparatus uses a two-stage pressure reservoir to accelerate a nylon piston into a titanium shaft positioned at the rear of a liquid-filled nozzle. Due to the high solubility of water in lithium fluoride, hexadecane ($C_{16}H_{34}$) was used as the impacting liquid. The rapid insertion of the shaft into the nozzle forces a high-velocity jet of liquid from the orifice onto the sample that is located on a computer-controlled *x-y* stage. The computer monitors the velocity of the jet of liquid as it emerges from the orifice.

In an earlier study, damage caused by these liquid jets was evaluated and compared with that resulting from impacts with spherical liquid drops (Ref 4). The rain erosion resistance of a material is characterized by determining its absolute damage threshold velocity (ADTV). This is the velocity below which, for a given liquid drop size, the sample will never experience any damage regardless of the number of impacts to which it is exposed. Due to the high accuracy of the MIJA jet velocity and positioning, this parameter can be simply obtained from a single-crystal sample. The sample (typically a 25 mm diameter disc) has up to fifteen sites selected on the surface with each site allocated an impact velocity. Each site was initially impacted once at that velocity and inspected for damage using an optical microscope at one hundred times magnification. The lowest velocity at which damage is observed after a single impact was recorded as damage threshold velocity (DTV) at one impact, i.e., the single-shot threshold velocity, and the sample was returned to the multiple impact jet apparatus so that each site can be impacted again. Impact damage was detected by inspecting the surface of impact using an optical microscope. After the crystal was impacted, it was etched to reveal dislocation movement and the formation of surface cracks. The samples were thoroughly washed in a solution of water and Teepol prior to etching the (001) surface. Once the sample

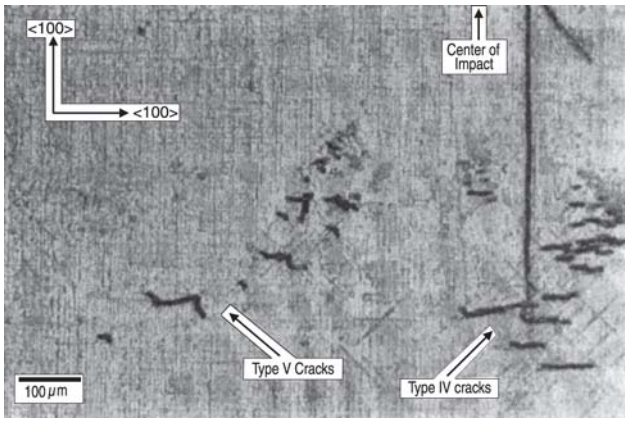

Fig. 4 Dislocation-etched (001) impact face of single-crystal lithium fluoride. Hexadecane was used to impact the surface at 200 m/s through a 0.8 mm diameter nozzle. The figure shows type IV cracks in the ⟨100⟩ radial direction, type V cracks to the left of type IV cracks, and a central impact crack some distance away from the center of impact.

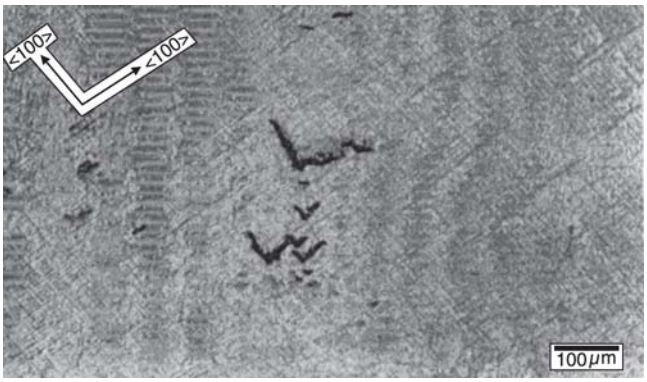

Fig. 5 Dislocation-etched (001) impact face of single-crystal lithium fluoride. Hexadecane was used to impact the surface at 200 m/s through a 0.8 mm diameter nozzle. The figure shows cracks that are apparent distortions in the radial direction of type II cracks. Intersections of these cracks from two quadrants form W-shaped cracks as shown.

was dried, hydrogen peroxide (H_2O_2) was used to reveal etch pits and regions of crack formation. Each sample was etched for 10 min at room temperature.

3. Experimental Results and Observations

The damage pattern observed after liquid impact on single-crystal lithium fluoride was typically a series of discrete circumferential cracks around an undamaged central zone. The cracks observed immediately outside the release radius are type III cracks that were used to detect the onset of the damage threshold. The pressure pulses produced by liquid impact are intense due to the compressible behavior of the liquid in the first stages of impact (Ref 5). Damage observed in single-crystal lithium fluoride was in the form of slip-band development in ⟨100⟩ direction until the material reached its damage threshold limit. At the damage threshold limit, a number of fractures and types of fracture are evident. In addition to type III cracks at the release radius, type IV cracks are observed in the ⟨100⟩ direction. Figure 4 shows type IV cracks to the right of the photograph. The cracks shown are variable in length; the largest emanates from the center of impact that, unusually, has a subsidiary crack running in the ⟨110⟩ direction. Referring to type III cracks, Adler (Ref 6) had shown that substantial surface and near-surface tensile stresses developed ahead of the shear wave in polycrystalline zinc sulfide just before the Rayleigh surface wave begins to develop. However, there was no evidence in the case of single-crystal lithium fluoride of subsurface tensile cracking associated with bulk waves. Type III cracks at the periphery of the impact zone did not have subsidiary cracks attached to them at trajectories associated with bulk waves. Although when one looks at a cross section of type IV cracks some distance away from the center of impact, there was evidence of subsurface tensile cracks that were presumably caused by the interaction of $\{110\}_{45^\circ}$ slip planes (Ref 7, 8).

Figure 4 also shows the existence of type V cracks. These cracks are apparent distortions of type II cracks in the radial ⟨110⟩ direction. Figure 5 shows the intersections of these cracks from two quadrants. They are typically W-shaped cracks and are associated with liquid impact on single-crystal materials, particularly magnesium oxide (Ref 3, 9). The increase in the number of W-shaped cracks occurred beyond the damage threshold limit of the material and was largely associated with the appearance of cracks in the ⟨100⟩ radial direction within the impact zone.

In some materials, repeated impact produces local failure on, or near, the impact axis. Bowden and Brunton (Ref 10) found this with polymethylmethacrylate (PMMA). In this case, the damage was located beneath the surface at a depth of about half the radius of the contact region R. This is where the Hertz theory for elastic contact would predict the maximum shear stress, and Bowden and Brunton (Ref 10) suggested this as an explanation. However, for loading that is dominated by a stress wave this is unlikely to be the full explanation. Experiments by Obara, Bourne, and Field (Ref 11) show that subsurface axial cracks in PMMA form when the release waves from the contact periphery interact giving net tension. Interestingly, the release waves will also travel in the liquid giving cavitation when they cross. The nuclei for such cavities could be the air trapped at the interface during impact. When the cavities themselves collapse, they could give peaks of high pressure that damage the surface. A third mechanism for damage at, or near, the central axis with polycrystalline materials is by the action of compressive or shear loading, which generates tensile failure at grain boundaries between grains depending on their orientation and anisotropy. Once a pit develops, hydraulic loading by trapped liquid can develop damage, as shown by Field (Ref 12). Central damage is likely to be less important than circumferential cracking in the rain erosion situation because it depends on multiple impacts on the same site. This situation can be simulated in the laboratory using MIJA but not by other techniques and only after very long exposures in the practical application.

Central impact damage in single-crystal lithium fluoride initially occurs as slip bands move, causing a "rippling" effect to be seen in the centrally loaded impact zone. As slip-band development continues after repeated impact, cracks begin to appear above the damage threshold limit, i.e., after type III and IV cracks have been established. Slip development leads to cracks predominantly in the [010] direction. As the severity of the impacts increases, cracking occurs in all principal ⟨100⟩ directions. These cracks are thought to be due to the interaction of $\{110\}_{45^\circ}$ slip planes (Ref 7, 8). Although there are many

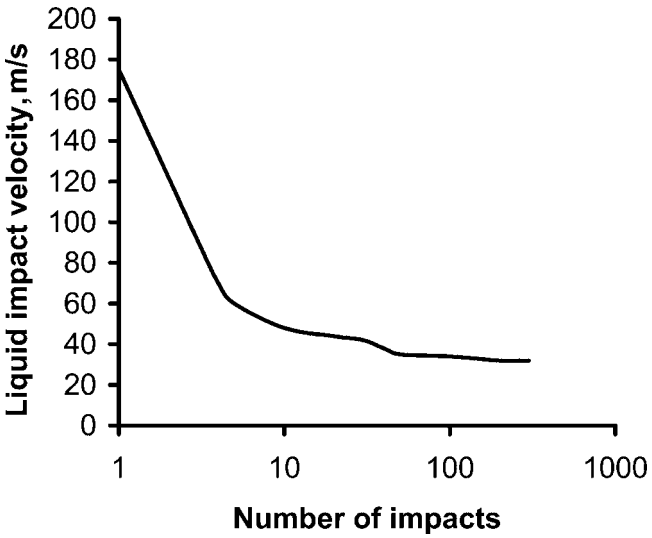

Fig. 6 Experimental damage threshold curve for single-crystal lithium fluoride. The single-shot threshold velocity from a 0.8 mm diameter nozzle is 175 m/s, while the damage threshold velocity after 300 impacts was 32 m/s.

explanations interpreting the effects of central impact damage in PMMA, the most likely explanation for central impact damage in single-crystal lithium fluoride is that hydrostatic compressive loading during impact enables subsurface slip bands to interact, i.e., shear interactions of slip planes. The slip planes, which have a greater tendency to slip, will do so thus causing a "rippling" effect on the surface of the impact site. As the severity of impact continues, {110} type cracks form due to the interaction of $\{110\}_{45^\circ}$ slip planes. It should be noted that Adler and James (Ref 3) did not observe cracks within the central impact region of single-crystal magnesium oxide. However, they did notice that slip plane interactions did occur within the central impact region but without crack formation. The damage threshold curve for single-crystal lithium fluoride subjected to multiple liquid impact is shown in Fig. 6. The single-shot threshold velocity from a 0.8 mm diameter nozzle was found to be 175 m/s, while the ADTV, i.e., DTV after 300 impacts, was 32 m/s.

4. Coated Materials

The resistance to fracture caused by water drop impact can be improved by applying a thin solid film to the substrate. Developments in the area of coating with boron phosphide, gallium phosphide, and diamond have provided significant improvements in raising damage thresholds in materials such as zinc sulfide, germanium, and glass materials. Developments in this area are reported in another paper.

5. Conclusions

The nature of impact damage in single-crystal lithium fluoride is typified by the appearance of type III cracks immediately at the release radius that are caused by the Rayleigh stress wave induced when a liquid drop impacts the (001) surface. At this limit, type IV cracks appear some distance away from the center of impact in the ⟨100⟩ radial direction. Type V cracks are also observed and are apparent distortions in the radial direction of type II cracks.

Central impact damage associated with single-crystal lithium fluoride occurred after several impacts on the same site above the damage threshold limit. These cracks are due to the interaction of $\{110\}_{45^\circ}$ slip planes.

Single-crystal lithium fluoride can be used as a model material to investigate the effect of multiple liquid impact on the development of cracks in materials.

References

1. K.H. Jolliffe, The Development of Erosion Damage in Metals by Repeated Liquid Impact, *Philos. Trans. R. Soc. London,* 1966, **A260,** p 101-108
2. M.J. Jackson and J.E. Field, "Liquid Impact Erosion of Single Crystal Magnesium Oxide," Paper 78, presented at *Proceedings of the 9th Conference on Erosion by Liquid and Solid Impact* (Churchill College, University of Cambridge), September 1998
3. W.F. Adler and T.W. James, "Localized Deformation and Fracture of Single Crystal Materials," *Fractography and Materials Science,* L.N. Gilbert and R.D. Zipp, Eds., American Society for Testing and Materials Publication No. STP 733, ASTM, 1981, p 271-290
4. R.J. Hand, J.E. Field, and D. Townsend, The Use of Liquid Jets to Simulate Angled Drop Impact, *J. Appl. Phys.,* 1991, **70,** p 7111-7118
5. F.P. Bowden and J.E. Field, The Brittle Fracture of Solids by Liquid Impact, Solid Impact and By Shock, *Proc. R. Soc. London,* 1964, **A232,** p 331-352
6. W.F. Adler, Liquid Drop Collisions on Deformable Media, *J. Mater. Sci.,* 1977, **12,** p 1253-1271
7. R.J. Stokes, T.L. Johnston, and C.H. Li, Deformation in Single Crystal Magnesium Oxide, *Philos. Mag.,* 1959, **4,** p 920-932
8. R.J. Stokes, T.L. Johnston, and C.H. Li, Mechanisms of Fracture in the Deformation of Magnesium Oxide, *Philos. Mag.,* 1960, **6,** p 9-24
9. M.J. Jackson and J.E. Field, Liquid Impact Erosion of Single Crystal Magnesium Oxide, *Wear,* 1999, **233-235,** p 39-50
10. F.P. Bowden and J.H. Brunton, The Deformations of Solids by Liquid Impact at Supersonic Speeds, *Proc. R. Soc. London,* 1961, **A263,** p 433-450
11. T. Obara, N.K. Bourne, and J.E. Field, Liquid Jet Impact on Liquid and Solid Surfaces, *Wear,* 1995, **186-187,** p 388-394
12. J.E. Field, "The Fracture and Deformation of Brittle Materials," Ph.D. dissertation, Cavendish Laboratory, University of Cambridge, U.K., 1962